

H 3-75: The Planetary Nebula with the Binary Central Star NSV 16624

V. P. Arkhipova¹, N. P. Ikonnikova^{1*}, M. A. Burlak¹, and A. V. Dodin¹

¹*Sternberg Astronomical Institute,
 Moscow State University, Universitetskii pr. 13, Moscow, 119234 Russia*

Received July 10, 2020; revised July 22, 2020; accepted July 23, 2020

Abstract—H 3-75 is a medium-excitation planetary nebula with a binary central star consisting of a hot subdwarf with $T_{\text{hot}} \sim 10^5$ K and a cool giant. We present the results of our photometric and spectroscopic observations obtained in 2020 and analyze data from the literature. The brightness of the cool component of the binary system has been measured in the VR_CI_CJHK bands. We have measured the relative intensities of emission lines in the spectrum of the planetary nebula H 3-75, estimated the extinction, and determined the gaseous envelope parameters. We have found the spectral type and luminosity class of the cool star to be K0 III and analyzed its spectrum. We have estimated the distance to the object ($d \sim 3660$ pc) and the luminosities of the components of the binary system: $L_{\text{cool}} \sim 50 L_{\odot}$ and $L_{\text{hot}} \sim 160 L_{\odot}$. The hot subdwarf's parameters T_{hot} and L_{hot} place the star on the cooling track of post-AGB stars.

DOI: 10.1134/S1063773720090017

Keywords: *planetary nebulae, photometric and spectroscopic observations, binary stars, evolution.*

INTRODUCTION

Searches for and studies of binary central stars in planetary nebulae (PNe) are extremely important both for explaining the morphology of PNe and for refining the Galactic scale of their distances. In most cases, the available statistical distance scales currently give a distance error up to 50%.

The Gaia mission has become a big breakthrough in determining the distances, including those to PNe. In the Gaia DR2 catalogue (2018) the parallaxes were determined for quite a few PNe, but the distance estimates from the parallaxes to PNe, which are mostly distant objects, require verification.

So far reliable individual distance determinations are available only for several tens of PNe, which is clearly insufficient to refine the zero point of the statistical distance scales. Therefore, new estimates of the individual distances to PNe from the components in binary nuclei must be welcomed.

PN H 3-75 = PN 193.6-09.5 with coordinates $05^{\text{h}}40^{\text{m}}45^{\text{s}}$ and $+12^{\circ}21'23''$ (2000) was discovered by Haro in 1953 (Haro et al. 1953). The diameter of its inner bright part is $24''$, this is a circular double-envelope nebula, the outer fainter part is traceable up to $70''$ from the center (Lutz and Lane 1987). A star with $m(pg) = 14^{\text{m}}$ is observed at the center of the nebula (Kogoutek 1985). The nebula has a high degree of excitation of its spectrum, as was shown

by Acker et al. (1992) and Kaler et al. (1996). The parameters of the nebula and its chemical composition have been determined repeatedly, in particular, by Kaler et al. (1996), Costa et al. (2004), Milanova and Kholtygin (2009), and Henry et al. (2010). H 3-75 with its spatial–kinematic characteristics and chemical composition belongs to the Peimbert PN type II (Quireza et al. 2007).

The photometric data on the central star are extremely scarce. In 1979–1981 Whitelock (1985) measured its JHK magnitudes, $J = 12^{\text{m}}13$, $H = 11^{\text{m}}50$, and $K = 11^{\text{m}}32$, with an accuracy of $\pm 0^{\text{m}}01$ and noted that the star could be variable in this range. In accordance with this assertion, the star was included in the catalogue of suspected variables under the number NSV 16624 without specifying the type of its variability. 2MASS provides the infrared (IR) brightness measurements performed on September 29, 1998: $J = 12^{\text{m}}00$, $H = 11^{\text{m}}46$, and $Ks = 11^{\text{m}}33$.

According to the private communication by Sanduleak (1984), the central star is very red; he estimated its spectral type as K.

The Hubble Space Telescope observations of H 3-75 (Ciardullo et al. 1999) within the program of searching for the binarity of PN nuclei did not reveal the binary's secondary component, while the magnitudes of NSV 16624 were obtained on August 18, 1993: $V = 14^{\text{m}}24$, $I_C = 13^{\text{m}}08$, and $(V - I)_C = +1.16$. The authors point out that their photometric measurements of the star are maximally free from

*E-mail: ikonnikova@gmail.com

Table 1. IR photometry for the comparison stars and the central star of PN H 3-75

ID 2MASS	J	H	K_S	$J(\text{MKO})$	$H(\text{MKO})$	$K(\text{MKO})$
05404316+1221320	13.788	13.372	13.326	13.757	13.360	13.311
05404760+1221445	13.651	13.206	13.195	13.621	13.193	13.181
05404531+1220232	13.870	13.407	13.315	13.833	13.398	13.298
05404688+1220115	12.966	12.772	12.730	12.951	12.760	12.721
05405020+1220154	12.856	12.529	12.415	12.827	12.521	12.401
05403648+1221162	12.680	12.375	12.237	12.650	12.368	12.223
05403776+1220142	12.602	12.252	12.134	12.571	12.244	12.119
05404497+1221225	12.042	11.481	11.379	11.997	11.472	11.363

the superposed PN emission background, while the accuracy of the estimates is $\pm 0^m02$.

Having the above-mentioned and our new photometric and spectroscopic data, in this paper we intend to refine the spectral type and luminosity class of the red component assuming that it is in pair with a hot star faint in optics, but ionizing the nebula H3-75. This refinement allowed us to determine the distance to the nebula and to estimate the luminosities of the components of the binary system. Furthermore, we propose to observers to carry out observations of the red component of the binary star to confirm or reject its suspected photometric variability.

OBSERVATIONS

IR Photometry

New observations of H 3-75 were obtained on March 10, 2020, (JD = 2458919.21) in the near-IR. The observations were carried out with the 2.5-m telescope at the Caucasus Mountain Observatory (CMO) of the Sternberg Astronomical Institute of the Moscow State University (SAI MSU) using the ASTRONIRCAM camera-spectrograph (Nadjip et al. 2017) in the direct imaging mode in the photometric JHK bands of the MKO system. The camera is equipped with a HAWAII-2RG 2048×2048 -pixel CCD detector. Only the central 1024×1024 -pixel part of the CCD array is efficiently used in photometric observations. A $4'6 \times 4'6$ region falls into the field of view of the detector.

Comparative photometry was performed with the Maxim DL-6 code. Stars from the 2MASS catalogue were used as standards. Table 1 lists the comparison stars with their magnitudes in the 2MASS and MKO systems. The magnitudes were

converted from 2MASS to MKO using the formulas from Leggett et al. (2006). The magnitudes derived by us for the central star of PN H 3-75, 2MASS05404497+1221225, from the March 10, 2020 observations are given in the last row of Table 1.

VR_CI_C Photometry

During three nights in March–April 2020 we imaged H 3-75 in three photometric bands of the Johnson–Cousins system, $VR_C I_C$. The observations were carried out with the 60-cm CMO SAI MSU reflector equipped with an Andor iKon-L CCD camera (2048×2048 pixels, a pixel size of $13.5 \mu\text{m}$, a scale of 0.67 arcsec per pixel) (for more details, see Berdnikov et al. 2020). The observations and primary data reduction, including the dark current subtraction, bias correction, and flat fielding, were carried out with the Maxim DL-6 code. Figure 1 shows a portion of the V image for PN H 3-75 obtained on March 28, 2020.

The magnitudes of the central star of PN H 3-75 were derived by comparison with the reference stars the data on which were taken from Dolan and Mathieu (2002) and are contained in Table 2. Based on the reference stars, for each pair of images in different bands we obtained the coefficients B of equations $M_i = B_0^{ik} \times m_i + B_1^{ik} \times m_k + B_2$, where m are the instrumental v , r , i magnitudes and M are the V , R_C , I_C magnitudes in the Johnson–Cousins system. Thus, for each band we obtained the pair of magnitudes in the Johnson–Cousins system calculated using the other two bands. For the field stars the discrepancies between them were no more than 0^m001 . Since all of the reference stars are located in the southern part of the field, the presence of a systematic error is not ruled out.

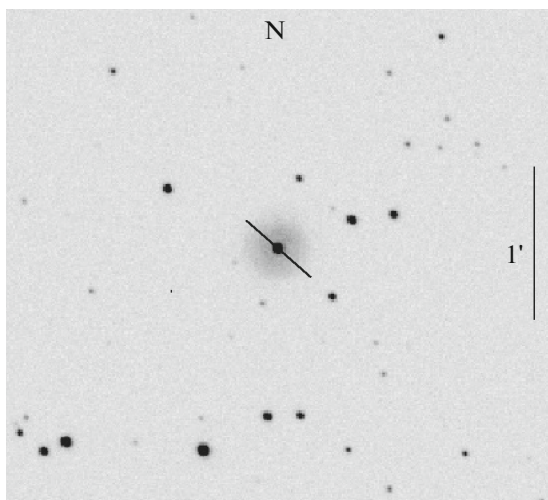


Fig. 1. Immediate neighborhoods of PN H 3-75 in the V band. The image was obtained on March 28, 2020. The slit position in our spectroscopic observations is shown in the image.

To determine the magnitudes of the central star, it was necessary to take into account the contribution from the nebula. The spectroscopic data presented below point to a ring shape of the nebula with a maximum brightness in [O III] and H I lines at a distance $r \sim 4''.8$ from the central star and an approximately linear brightness decline from the maximum to the center and to the periphery. We constructed the nebula's radial brightness profile by averaging the counts in concentric rings about $0''.75$ in thickness with the center coincident with the central star. The nebula's brightness profile was then fitted by a linear function in the range $4''.8$ – $28''.5$. The brightness of the nebula's inner region ($r < 4''.8$) was calculated by assuming its

decline from $r = 4''.8$ to the center to be symmetric to the decline from $r = 4''.8$ outward. The calculated brightness distribution of the nebula was subtracted from the composite image and then the radiation from the central star was measured. For comparison, we also measured the total radiation from the star and the nebula in the same aperture. The contribution from the nebula was $0^m.27$, $0^m.1$, and $0^m.03$ in the V , R_C , and I_C bands, respectively. This may be considered as an upper limit for the error in the magnitudes of the central star. The instrumental magnitudes of the PN nucleus were then converted to the Johnson–Cousins system using the coefficients B considered in the previous section.

Data on the photometry for the central star of PN H 3-75 are given in Table 3. The root-mean-square deviation per night is specified as an error.

Spectroscopic Observations

Our spectroscopic observations of H 3-75 were carried out on March 3, 2020, at the 2.5-m CMO SAI MSU telescope with a low-resolution double-beam spectrograph. The instrument is described in detail in Potanin et al. (2020). Andor Newton 940P cameras with 512×2048 -pixel E2V CCD42-10 CCD are used as detectors. The observations were performed with a long $1''.0$ -wide slit in the spectral range $\lambda 3500$ – 7500 . The slit was put vertically toward the zenith to minimize the influence of atmospheric refraction. The position angle was 40° (Fig. 1). Three frames were taken with an exposure time of 600 s each. The data reduction included the bias correction, flat fielding, and dark current subtraction. Cosmic-ray particle hits were removed from the two-dimensional spectrogram. To make a correction for the spectral sensitivity of the detector, we observed the spectra of the standard BD+75°325.¹ The one-dimensional spectra were obtained by summing the counts within an 80-pixel ($30''$) aperture. The data were reduced using self-developed Python scripts.

ANALYSIS OF THE SPECTRUM FOR PN H 3-75 AND ITS CENTRAL STAR NSV 16624

Emission lines typical of medium- and high-excitation PNe are observed in the spectrum of PN H 3-75 in the range $\lambda 3500$ – 7500 . Figure 2 shows the composite spectrum of PN H 3-75 and its central star NSV 16624.

We measured the relative intensities of nebular emission lines and give them in Table 4 with the corresponding data from Kaler et al. (1996) and Henry

Table 2. VR_CI_C photometry for the reference stars

Designation	V	R_C	I_C
J054025.7+121142	13.974	13.230	12.570
J054037.0+121204	12.483	11.913	11.437
J054040.1+121106	13.269	12.540	11.883
J054040.9+121035	12.848	12.330	11.858
J054044.4+121034	13.907	13.381	12.896
J054048.1+121128	14.674	14.303	13.930
J054052.3+121113	14.983	14.326	13.715
J054110.2+121149	14.386	13.916	13.432

¹ <https://www.eso.org/sci/observing/tools/standards/spectra/stanlis.html>.

Table 3. VR_CI_C photometry for NSV 16624

Date	JD	V	R_C	I_C
Mar. 9, 2020	2458918.288	14.318 ± 0.003	13.655 ± 0.019	13.020 ± 0.011
Mar. 28, 2020	2458937.204	14.333 ± 0.013	13.660 ± 0.010	13.007 ± 0.005
Apr. 3, 2020	2458943.207	14.335 ± 0.009	13.665 ± 0.005	13.016 ± 0.013

Table 4. The observed relative intensities of emission lines of PN H 3-75 in the scale $F(H\beta) = 100$ from the published data and our new observations

λ , Å	Species	$F(\lambda)$, Kaler et al. (1996)	$F(\lambda)$, Henry et al. (2010)	$F(\lambda)$, this paper
3727-29	[O II]	—	80 ± 22	157 ± 11
3868.8	[Ne III]	—	68 ± 17	87 ± 5
3889.1	H8	—	16 ± 4	16 ± 2
3970.1	H7 + [Ne III]	—	37 ± 8.7	39 ± 2
4101.7	H δ + He II	—	20.3 ± 4.6	21 ± 2
4340.5	H γ	—	43 ± 8.1	44 ± 3
4363.2	[O III]	—	11 ± 2	18 ± 3
4685.7	He II	42.5	25 ± 3.8	23 ± 2
4861.3	H β	100	100	100.00
4959.5	[O III]	393	400 ± 54	379 ± 15
5007.6	[O III]	1183	1300 ± 170	1147 ± 46
5875.6	He I	30.6	15 ± 1.6	13 ± 1
6548.1	[N II]	—	28 ± 3.2	28 ± 1
6562.9	H α	375	360 ± 1	335 ± 10
6583.4	[N II]	46.2	86 ± 9.8	85 ± 3
6678.2	He I	—	4.1 ± 0.48	4.1 ± 0.9
6716.4	[S II]	—	18 ± 2.1	16.4 ± 0.8
6730.8	[S II]	—	14 ± 1.6	12.7 ± 0.5
7065.2	He I	—	2.8 ± 0.34	2.4 ± 0.3
7136.2	[Ar III]	12.5	16 ± 2	16.4 ± 0.7
7320.0	[O II]	—	4.7 ± 0.59	3.4 ± 0.4
7330.0	[O II]	—	—	0.8 ± 0.4

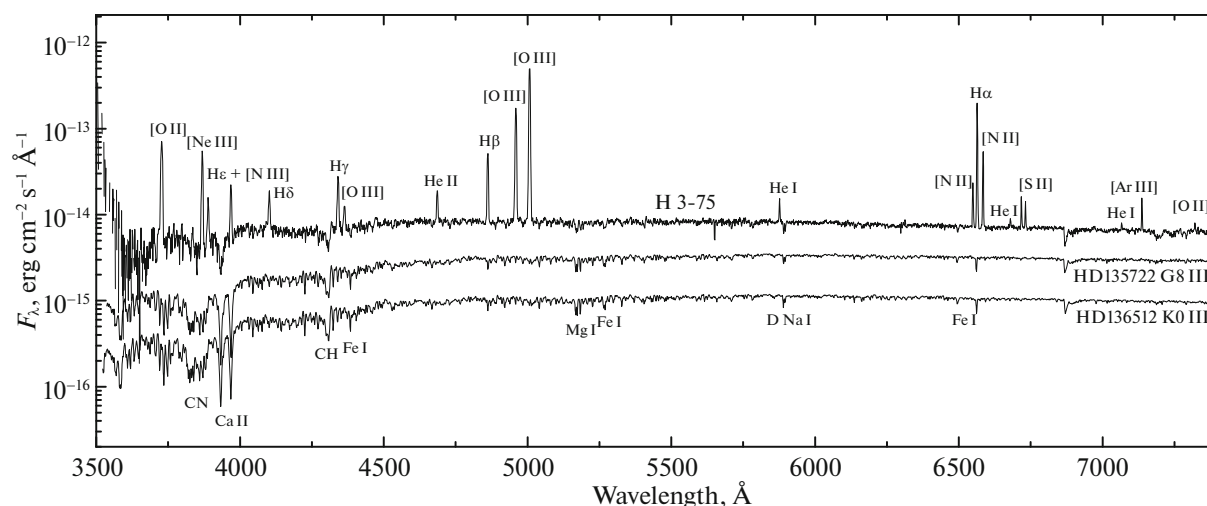


Fig. 2. Dereddened combined spectrum of PN H 3-75 and its central star NSV 16624 together with the spectra of the giants HD 136512 and HD 135722 shifted arbitrarily relative to the vertical axis.

et al. (2010). The relative intensities for a number of lines presented in Costa et al. (2004) are already corrected for reddening, therefore, we did not place them in Table 4 along with the observational data.

Our measurements are in good agreement with the data from Henry et al. (2010), obtained closest to our observations. The relative intensity of the [O II] $\lambda 3727\text{--}3729$ doublet is an exception: our estimate is almost twice that of Henry et al. (2010). The relative intensities of the nebular [O III] lines derived by different authors agree satisfactorily, while the data for the He II $\lambda 4686$ line differ by an order of magnitude: from 0.031 (Costa et al. 2004) to 0.4 (Kaler et al. 1996). These differences are related primarily to different techniques of observations. The observations by Kaler et al. (1996) were carried out with a circular $8''$ aperture and refer to the central part of the nebula. Costa et al. (2004) and Henry et al. (2010) observed the nebula with a long $2''$ -wide slit; our measurements refer to a $1'' \times 30''$ aperture.

Figure 3 shows the intensity distribution along the slit in the He II $\lambda 4686$, $H\beta$, [O III] $\lambda 5007$, $H\alpha$, [N II] $\lambda 6584$, and [S II] $\lambda 6716$ lines. The graph allows the angular size of the nebula in different lines to be estimated and illustrates the fact that the nebula is ring-like and asymmetric in the He I, [O III], [N II], and [S II] lines, while in the He II $\lambda 4686$ line a concentration to the center of the nebula is clearly seen. In the central part of the nebula the $H\beta$ emission is weaker and the ratio $F(\lambda 4686)/F(H\beta)$ is larger than those in other regions. Apparently, this explains the high relative intensity of the ionized helium line in Kaler et al. (1996). The low value of this quantity in Costa et al. (2004) is perplexing. The hydrogen and O^{+2} emission zones virtually coincide and, therefore, the relative intensities of the [O III] $\lambda 4959$ and $\lambda 5007$

lines derived by different authors are in good agreement.

A large scatter of relative He I and He II line intensities led to a discrepancy in total helium abundance in the nebula in different papers. Kaler et al. (1996), Costa et al. (2004), Milanova and Kholtygin (2009), and Henry et al. (2010) give $He/H = 0.22$, 0.071 , 0.08 , and 0.120 ± 0.014 , respectively.

We estimated the interstellar reddening toward H3-75 from the Balmer decrement of the nebula: the observed relative intensities $F(H\alpha) : F(H\beta) : F(H\gamma) = 3.35 : 1 : 0.44$ were referred to the theoretical ones from Storey and Hummer (1987) $I(H\alpha) : I(H\beta) : I(H\gamma) = 2.86 : 1 : 0.47$ for $T_e = 10000$ K and $N_e = 100 \text{ cm}^{-3}$. The value of $c(H\beta) = 0.21$ was obtained. Previously, from the measured intensity ratio of the $H\alpha$ and $H\beta$ lines Tyllenda et al. (1992), Kaler et al. (1996), and Henry et al. (2010) derived $c(H\beta) = 0.5$, 0.36 , and 0.28 , respectively. Taking into account all the estimates, we obtained the mean $E(B - V) = 1.46c(H\beta) = 0.23 \pm 0.08$, which will be used below.

We determined the physical parameters of the nebula using the Pyneb package (Luridiana et al. 2015). The electron density $n_e \sim 230 \text{ cm}^{-3}$ was derived from the intensity ratio of the forbidden [S II] lines $R_{S2} = I(\lambda 6716)/I(\lambda 6731) = 1.29 \pm 0.11$; the electron temperature in the [O III] line formation zone $T_e = 14000 \pm 1300$ K was estimated from the ratio $R_{O3} = (I(\lambda 4959) + I(\lambda 5007))/I(\lambda 4363) = 74.5 \pm 12$.

To estimate the total helium abundance in the nebula, we used the reddening-corrected line intensity ratios $I(\lambda 4686)/I(H\beta) = 0.24$, $I(\lambda 5876)/I(H\beta) = 0.11$, $I(\lambda 6678)/I(H\beta) = 0.03$ and the formulas from Izotov et al. (1994). We obtained $He/H =$

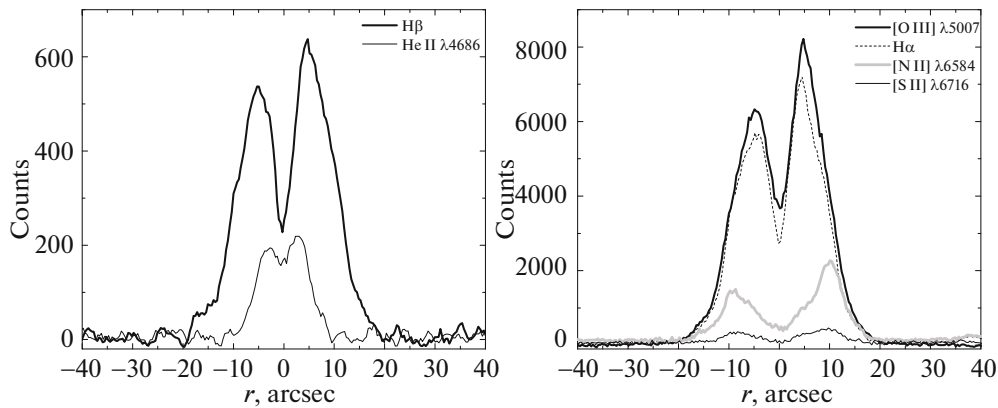


Fig. 3. Intensity distribution along the slit in the He II $\lambda 4686$, H β , [O III] $\lambda 5007$, H α , [N II] $\lambda 6584$, and [S II] $\lambda 6716$ lines.

$\text{He}^{2+}/\text{H}^+ + \text{He}^+/\text{H}^+ = 0.021 + 0.087 = 0.11 \pm 0.02$, which agrees with the value determined by Henry et al. (2010).

Let us now turn to the spectrum of the cool component of the central star of H 3-75 dominating in the optical range. For the spectral classification we compared the dereddened spectrum of NSV 16624 with the spectra of several stars of different spectral types and luminosity classes: HD 175305 (G5 III), HD 135722 (G8 III), HD 136512 (K0 III), HD 137759 (K2 III), HD 075732 (G8 V), HD 041593 (K0 V), HD 48329 (G8 I) from the library of stellar spectra ($R \sim 2000$) by Le Borgne et al. (2003) and HD 186293 (K0 I) from the library of stellar spectra by Jacoby et al. (1984). NSV 16624 has less intense metal lines than do the main-sequence stars HD 075732 and HD 041593. Its spectral energy distribution differs significantly from that for the K2 giant HD 137759 and the supergiants HD 48329 and HD 186293. At the same time, as shown in Fig. 2, NSV 16624 is also similar to G8 and K0-type giants in spectral features and overall energy distribution.

Given that the optically observed component of NSV 16624 is orbiting a highly evolved star, the true PN nucleus, it was important to check whether this neighborhood affected the atmospheric chemical composition of the cool giant. We know a number of PNe with binary central stars, in particular, LoTr 5 (Thévenin and Jasniewicz 1997), A 70 (Miszalski 2012), WeBo1 (Bond et al. 2003), and Hen 2-39 (Bond et al. 2013), that contain a G- or K-type subgiant or giant with an enhanced barium abundance as the cool component of the binary system. The Ba II $\lambda 4554$ line was detected in the spectra of these stars and, in some cases, the Ba II $\lambda 6142$, $\lambda 6497$, and Sr II $\lambda 4216$ lines are present, suggesting that the atmosphere of the cool giant is “polluted” with matter from the second component in the common-envelope phase.

Figure 4 shows the regions of the spectrum for NSV 16624 in which the Ba II $\lambda 4554$, $\lambda 4934$, $\lambda 5854$, $\lambda 6142$, $\lambda 6497$ and Sr II $\lambda 4216$ could be detected. For comparison, Fig. 4 also presents fragments of the spectrum for the barium star HD 49641 (Sp K0 I) from the ELODIE V3.1 library (Prugniel et al. 2007). The echelle spectrum of HD 49641 was smoothed by a moving average filter with $N = 17$. It can be seen that the Ba II $\lambda 4554$ line is absent in the spectrum of NSV 16624, the Ba II $\lambda 4934$, $\lambda 5854$, $\lambda 6142$, and Sr II $\lambda 4216$ absorptions, if any, are very weak. Observations of a better resolution than ours are needed to resolve the Ba II $\lambda 6497$ blend with Fe I $\lambda 6495$. It can be tentatively concluded that the cool star has not been strongly contaminated by its companion. High-resolution spectroscopic observations are needed for greater reliability.

PARAMETERS OF THE COOL COMPONENT AND THE DISTANCE TO THE NEBULA

The reddening-corrected spectrum of NSV 16624 shows a similarity to the spectra of G8 and K0 giants. For a more accurate spectral classification it is necessary to consider the spectral energy distribution in a wider spectral range by eliminating the influence of the nebular continuum. For this purpose, we use our $VR_C I_C JHK$ photometry.

To compare the spectral energy distribution of NSV 16624 with the data for standard stars from Straižys et al. (1979) in the optical range and Koornneef (1983) in the near-IR, we converted our observations in the R_C and I_C bands to R and I using the equations from Bessell (1979) and the JHK_S magnitudes in the 2MASS system to JHK from Koornneef (1983) using the formulas by Carpenter (2001).

As shown above, the color excess inferred from our spectroscopic data has a significant uncertainty of 0.08. We compared the spectral energy distribution from our broadband photometry for NSV 16624

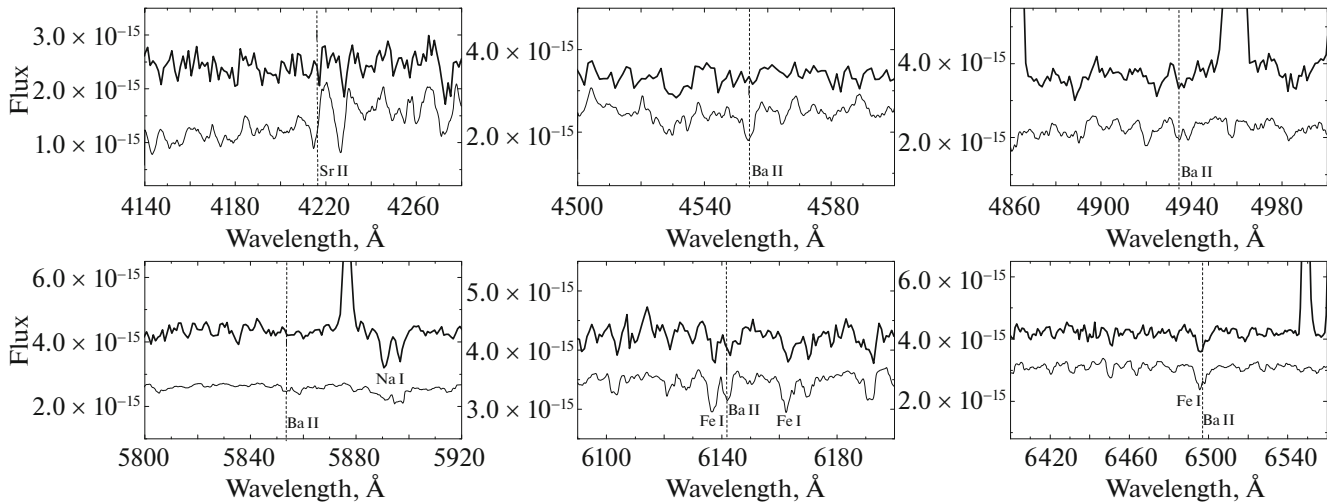


Fig. 4. Fragments of the spectra for NSV 16624 (thick line) and HD 49641 (thin line). The vertical dashed lines indicate the positions of the absorptions of interest to us. The spectrum of HD 49641 is shifted arbitrarily along the vertical axis.

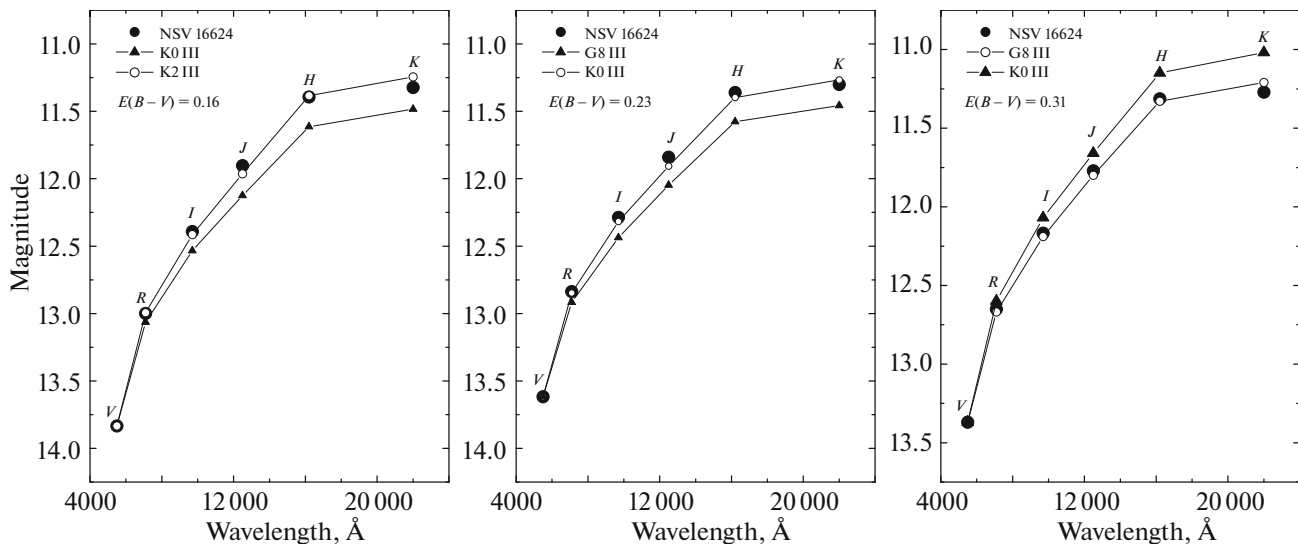


Fig. 5. Spectral energy distribution of NSV 16624 for various values of $E(B - V)$ and standard G8, K0, and K2 giants.

dereddened with three values of $E(B - V)$ (0.16, 0.23, and 0.31—the minimum, intermediate, and maximum ones) with the spectral energy distribution for standard giants of spectral types G8, K0, and K2 in the calibrations by Straizys (1979) and Koorneef (1983). As can be seen from Fig. 5, the spectral energy distribution in the $VR I J H K$ bands for NSV 16624 corresponds to K2 III for $E(B - V) = 0.16$, K0 III for $E(B - V) = 0.23$, and G8 III for $E(B - V) = 0.31$.

According to the interstellar extinction maps (Green et al. 2019), the color excess toward H 3-75 for a distance $d > 1500$ pc is $E(B - V) = 0.24^{+0.03}_{-0.01}$ and does not exceed $E(B - V) = 0.27$. H 3-75 has

no far-IR excess and, consequently, no circumstellar extinction. On the one hand, this gives grounds to believe that $E(B - V) = 0.31$ is slightly overestimated and, consequently, NSV 16624 has a later spectral type than G8 III. On the other hand, the spectral type K2 III deduced for $E(B - V) = 0.16$ relates poorly to the spectral energy distribution of NSV 16624 in the short-wavelength range; consequently, this value of $E(B - V)$ is underestimated and the star has an earlier spectral type. Thus, we think that the spectral type K0 III may be adopted for NSV 16624. According to the calibrations by Straizys (1982), the temperature of a K0 giant is $T_{\text{eff}} = 4797$ K. Given some uncertainty in the estimate of the spectral type

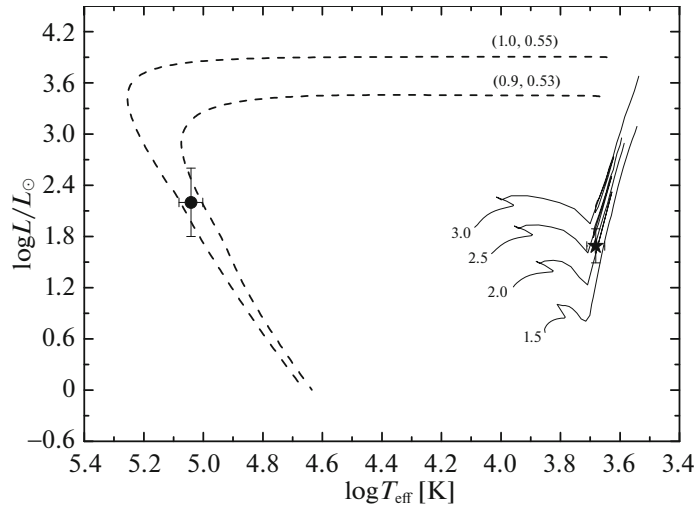


Fig. 6. Positions of the cool (star) and hot (circle) components of the binary system on the Hertzsprung–Russell diagram. The solid lines indicate the evolutionary tracks for initial masses of 1.5, 2.0, 2.5, and 3.0 M_{\odot} from Schaller et al. (1992). The dashed lines indicate two models by Miller Bertolami (2016) (M_{init} , M_{fin}).

for NSV 16624, we will adopt $T_{\text{eff}} = 4800 \pm 200$ K for the star.

Adopting the absolute magnitude $M_V = +0^m.8$ for K0 III (Straizys 1982) and using our estimate of the magnitude for NSV 16624 $V = 14^m.33$ and the color excess $E(B - V) = 0.23 \pm 0.08$, we derived the distance to the nebula $d = 3659^{+443}_{-394}$ pc and its height above the Galactic plane $z = -608^{+65}_{-74}$ pc. The diameter of the planetary nebula is $D \sim 0.50$ pc and its radius is $R \sim 0.25$ pc, suggesting a rather late expansion stage of the nebula. The bolometric absolute magnitude of a K0 giant is $M_{\text{bol}} = +0^m.5$ (Straizys 1982) and its luminosity is $\log L/L_{\odot} = 1.69$.

Amnuel et al. (1984) found the distance to H 3-75 in their statistical PN distance scale to be 2700 pc and its diameter to be 0.31 pc. The Gaia DR2 catalogue (2018) provides the measured parallax of the central star NSV 16624 of PN H 3-75, 0.2308 ± 0.0386 mas, while Bailer-Jones et al. (2018) estimated the distance from Gaia DR2 data to be $d = 3687^{+600}_{-462}$ pc. Our estimate of $d = 3659^{+443}_{-394}$ pc virtually coincides with the distance deduced from the parallax.

THE EXCITATION CLASS OF PN H 3-75, THE TEMPERATURE AND LUMINOSITY OF THE EXCITING STAR

According to the criteria by Feast (1968) and Morgan (1984), H 3-75 belongs to medium-excitation PNe and with its ratio $I(4686)/I(\text{H}\beta) = 0.24\text{--}0.40$ has an excitation class $EC = 5.7\text{--}6.4$ (Dopita and Meatheringham 1990). If, however, we take into

account the ratio $I(\text{H}\beta)/I(3869) = 5.1$, which Morgan (1984) uses as an additional criterion, then H 3-75 may be attributed to lower-excitation nebulae.

Preite-Martinez et al. (1991) determined the temperature of the exciting star of H 3-75 by the energy-balance method, $T_{\text{EB}} = 99\,800$ K. We estimated the temperature by Ambartsumyan’s method from the intensity ratio of the He II $\lambda 4686$ and $\text{H}\beta$ lines to be $T_{\text{HeII}} = 120\,000$ K. We will adopt the mean $T_{\text{hot}} = 110\,000 \pm 10\,000$ K.

Next, let us estimate the luminosity of the exciting star. In the visible range it is difficult to separate its contribution from the total radiation of the binary system (cool star + hot star + gas continuum) and, therefore, we used data from the International Ultraviolet Explorer (IUE) in the ultraviolet (UV) range, where only the hot star radiates. The low-resolution spectrum SWP34711 was taken on November 8, 1988, with the short-wavelength SWP camera covering the range 1150–3200 Å and extracted by us using the INES archive data server.² It should be noted that the UV flux is extremely low and is estimated unreliably. We calculated the visible flux using the flux at 1500 Å $F(\lambda 1500) \sim 3.4 \times 10^{-15}$ erg cm⁻² s⁻¹ Å⁻¹ and assuming the hot star to radiate as a blackbody with $T = 110\,000$ K, for which $k = I(\lambda 1500)/I(\lambda 5450) = 123$. Given the extinction of $E(B - V) = 0.23$, we obtained $F(\lambda 5450) \sim 8.1 \times 10^{-17}$ erg cm⁻² s⁻¹ and $V \sim 19^m.2$. For the distance $d = 3660$ pc and bolometric correction $BC = -6^m.4$ inferred from the formula $BC = 27.58 - 6.8 \log T_{\text{eff}}$

² <http://sdc.cab.inta-csic.es/cgi-ines/IUEdbsMY>

Table 5. IR photometry for NSV 16624

Date	J	H	K_S	Source
1979–1981	12.03	11.48	11.33	Whitelock (1985)
Sep. 29, 1998	11.999	11.451	11.303	2MASS
Oct. 3, 2020	12.042	11.481	11.379	This paper

from Martins et al. (2005), we estimated the luminosity of the hot star to be $\log L/L_\odot \sim 2.2$.

Figure 6 shows the positions of both components of the binary system on the Hertzsprung–Russell diagram together with the evolutionary tracks from Schaller et al. (1992) for initial masses of 1.5, 2.0, 2.5, 3.0 M_\odot and two models by Miller Bertolami (2016) for post-AGB stars: $M_{\text{init}} = 0.9 M_\odot$, $M_{\text{fin}} = 0.53 M_\odot$ and $M_{\text{init}} = 1.0 M_\odot$, $M_{\text{fin}} = 0.55 M_\odot$, where M_{init} is the mass on the zero-age main sequence and M_{fin} is the mass at the post-AGB stage. A comparison with the model tracks allowed us to estimate the masses of the hot and cool stars of the binary system, $M_{\text{hot}} = 0.53\text{--}0.55 M_\odot$ and $M_{\text{cool}} \sim 2 M_\odot$, and the mass of the progenitor of the hot star on the zero-age main sequence, $M_{\text{init}} = 0.9\text{--}1.0 M_\odot$.

According to the models by Miller Bertolami (2016), the evolution time of the star from the end of the AGB stage to the present time is $\sim 12\,000$ yr or 3.8×10^{11} s. Given the radius and lifetime of the nebula formed at the end of the AGB stage, let us estimate the expansion velocity of the nebula. It is found to be $V_{\text{exp}} \sim 20 \text{ km s}^{-1}$, which is consistent with the known data on the expansion velocities of planetary nebulae, especially at their late stages.

ON THE POSSIBLE PHOTOMETRIC VARIABILITY OF THE CENTRAL STAR NSV 16624

One component of the central star of the nebula, the red giant, was suspected of photometric variability in the JHK bands based on the observational data obtained in 1979–1981 (Whitelock 1985).

Let us compare the data referring to different epochs. To compare the IR magnitudes measured by Whitelock (1985) in the photometric SAAO system, we reduced them to the photometric 2MASS system using the equations derived by Carpenter (2001) and give them in Table 5 together with the 2MASS data and our new measurements.

While considering all of the presented photometry, we have not yet obtained evidence of near-IR photometric variability for NSV 16624. We have showed that the cool component, a normal giant, is outside

the instability strip and one should not expect periodic brightness variations caused by pulsations from it.

Nevertheless, in the case of a favorable orbit orientation in the plane of the sky the binary star at the center of PN H 3-75 could exhibit a periodic optical variability related to the orbital motion.

There are very little accurate photometric data for the optical range. In the literature there exists only one magnitude estimate for NSV 16624 in the V and I_C bands obtained by converting the fluxes at 5550 and 7850 Å measured by the Hubble satellite (Ciardullo et al. 1999). In this paper we provide the brightness of the central star in the VR_CI_C bands during three nights of observations. So far no brightness variations exceeding the observational, measurement, and reduction errors have been detected. A long monitoring is required for the detection of variability. The observations should be carried out in the I or I_C bands, in which the contribution from the nebula is minimal.

An analysis of the ASAS-SN observations (Shappee et al. 2014; Kochanek et al. 2017) in the V band from January 20, 2012, to November 29, 2018, (more than 500 estimates) showed no periodic brightness variations in the star. Chaotic brightness variations with an amplitude up to $0^m.1$ per night at a mean measurement accuracy of $0^m.02$ are observed. The object's mean brightness from the ASAS-SN data is $V = 13^m.31 \pm 0^m.03$ and exceeds significantly (by $\sim 1^m$) the brightness of the central star. Given the ASAS-SN CCD scale of 7.8 aecsec/pixel and $16''$ spatial resolution, the aperture photometry performed in the survey measures the total radiation from the star and the nebula. Observations with a better spatial resolution and a more rigorous allowance for the background are needed for careful photometry of objects with envelopes.

DISCUSSION AND CONCLUSIONS

Based on the published and newly acquired photometric and spectroscopic data on PN H 3-75 and its central star, we showed that the latter could be a binary consisting of a normal K0 III giant and a hot subdwarf with a temperature $\sim 10^5$ K. Our estimate of

the distance to the cool component of the binary system $d \sim 3660$ pc virtually coincides with the distance determined from the parallax. The mass of the giant was estimated by a comparison with the evolutionary tracks to be $M_{\text{cool}} \sim 2 M_{\odot}$. By assuming the central star of PN H 3-75 to be a physical pair, we determined the luminosity of the hot component of the binary system and concluded that the subdwarf is on the cooling track. Note, however, that no nucleosynthesis products of the hot component were detected in the spectrum of the cool star. This may suggest that the binary system is not bound physically or the pair is wide.

Ciardullo et al. (1999) hypothesized that the central star of PN H 3-75 could be a single one and evolve back to the AGB as a result of the last helium shell flash. The observational data obtained to date give no grounds for such a conclusion. As regards the Hertzsprung-Russell diagram, the cool star's parameters, $\log T_{\text{eff}}$ and $\log L/L_{\odot}$, place the star on the red giant branch before the AGB stage. A star evolving back to the AGB should have a considerably higher luminosity and a changed chemical composition. For example, the atmosphere of the star FG Sge in a stage after the last helium flash is significantly enriched with s-process elements (Jeffery and Schönberner 2006), while we detected neither barium nor strontium lines in the spectrum of NSV 16624. Consequently, PN H 3-75 is the product of the evolution of the hot component and not of the cool star.

The cool star is yet to traverse its path first in the red giant stage and then on the AGB, where the star will begin to intensively lose its mass. By this time the planetary nebula H 3-75 will disperse, while the hot component of the binary system will continue to evolve along the cooling track. The subsequent history depends on the mass loss rate of the cool component and on the scenario of mass transfer to the white dwarf.

In conclusion, we once again point out the need for a photometric monitoring of the central star of PN H 3-75 to detect a periodic variability related to the orbital motion. It is important to obtain high-resolution spectroscopy for the central star NSV 16624 to determine its atmospheric parameters and chemical composition. UV observations of the object are vital for a more accurate determination of the parameters of the hot star, the true nucleus of PN H 3-75.

FUNDING

This study was performed using the equipment purchased through the funds of the Program for the Development of the Moscow State University.

REFERENCES

1. A. Acker, F. Ochsenbein, B. Stenholm, R. Tylenda, J. Marcout, and C. Schohn, *Strasbourg-ESO Catalogue of Galactic Planetary Nebulae* (ESO, Strasbourg, 1992).
2. P. Amnuel, O. Guseinov, K. Novruzova, and I. S. Rustamov, *Astrophys. Space Sci.* **107**, 19 (1984).
3. C. A. L. Bailer-Jones, J. Rybizkii, M. Fouesneau, G. Mantelet, and R. Andrae, *Astron. J.* **156**, 58 (2018).
4. L. N. Berdnikov, A. A. Belinskii, N. I. Shatskii, M. A. Burlak, N. P. Ikonnikova, E. O. Mishin, D. V. Cheryasov, and S. V. Zhuiko, *Astron. Rep.* **64**, 310 (2020).
5. M. S. Bessell, *Publ. Astron. Soc. Pacif.* **91**, 589 (1979).
6. H. E. Bond, D. L. Pollacco, and R. F. Webbink, *Astron. J.* **125**, 260 (2003).
7. J. F. le Borgne, G. Bruzual, R. Pelló, A. Lançon, B. Rocca-Volmerange, B. Sanahuja, D. Schaerer, C. Soubiran, and R. Vilchez-Gomez, *Astron. Astrophys.* **402**, 433 (2003).
8. A. G. A. Brown, A. Vallenari, T. Prusti, et al. (Gaia Collab.), *Astron. Astrophys.* **616**, 10 (2018).
9. J. M. Carpenter, *Astron. J.* **121**, 2851 (2001).
10. R. Ciardullo, H. Bond, M. Sipior, L. Fullton, C.-Y. Zhang, and K. G. Schaefer, *Astrophys. J.* **118**, 488 (1999).
11. R. Costa, M. Ushida, and W. Maciel, *Astron. Astrophys.* **423**, 199 (2004).
12. C. J. Dolan and R. D. Mathieu, *Astron. J.* **123**, 387 (2002).
13. M. A. Dopita and S. J. Meatheringham, *Astrophys. J.* **357**, 140 (1990).
14. M. W. Feast, *Mon. Not. R. Astron. Soc.* **140**, 345 (1968).
15. G. M. Green, E. Schlafly, C. Zucker, J. S. Speagle, and D. Finkbeiner, *Astrophys. J.* **887**, 93 (2019).
16. G. Haro, B. Iriarte, and E. Chavira, *Bol. Observ. Tonantzintla Tacubaya* **1** (8), 3 (1953).
17. R. B. Henry, K. Kwitter, A. Jasket, B. Balik, M. A. Morrison, and J. B. Milingo, *Astrophys. J.* **724**, 748 (2010).
18. Y. I. Izotov, T. X. Thuan, and V. A. Lipovetsky, *Astrophys. J.* **435**, 647 (1994).
19. G. H. Jacoby, D. A. Hunter, and C. A. Christian, *Astrophys. J. Suppl. Ser.* **56**, 257 (1984).
20. C. S. Jeffery and D. Schönberner, *Astron. Astrophys.* **459**, 885 (2006).
21. J. Kaler, K. Kwitter, R. Shaw, and L. Browning, *Publ. Astron. Soc. Pacif.* **108**, 980 (1996).
22. C. S. Kochanek, B. J. Shappee, K. Z. Stanek, T. W.-S. Holoiien, T. A. Thompson, J. L. Prieto, S. Dong, J. V. Shields, D. Will, C. Britt, D. Perzanowski, and G. Pojmanski, *Publ. Astron. Soc. Pacif.* **129**, 104502 (2017).
23. L. Kogoutek, *Astron. Astrophys. Suppl. Ser.* **60**, 87 (1985).
24. J. Koornneef, *Astron. Astrophys.* **128**, 84 (1983).

25. S. K. Leggett, M. J. Currie, W. P. Varricatt, T. G. Hawarden, A. J. Adamson, J. Buckle, T. Carroll, J. K. Davies, et al., *Mon. Not. R. Astron. Soc.* **373**, 781 (2006).
26. V. Luridiana, C. Morisset, and R. A. Shaw, *Astron. Astrophys.* **573**, 42 (2015).
27. J. Lutz and Jo Lamé, in *Proceedings of the 131st IAU Symposium on Planetary Nebulae: Observations and Theory*, Ed. by S. Torres-Peimbert (Dordrecht, Reidel, 1989).
28. F. Martins, D. Schaerer, and D. J. Hillier, *Astron. Astrophys.* **436**, 1049 (2005).
29. Yu. V. Milanova and A. F. Kholtygin, *Astron. Lett.* **35**, 518 (2009).
30. M. M. Miller Bertolami, *Astron. Astrophys.* **588**, 25 (2016).
31. B. Miszalski, H. M. J. Boffin, D. J. Frew, A. Acker, J. Köppen, A. F. J. Moffat, and Q. A. Parker, *Mon. Not. R. Astron. Soc.* **419**, 39 (2012).
32. B. Miszalski, H. M. J. Boffin, D. Jones, A. I. Karakas, J. Köppen, A. A. Tyndall, S. S. Mohamed, P. Rodriguez-Gil, and M. Santander-Garcia, *Mon. Not. R. Astron. Soc.* **436**, 3068 (2013).
33. D. H. Morgan, *Mon. Not. R. Astron. Soc.* **208**, 633 (1984).
34. A. E. Nadzhip, A. M. Tatarnikov, D. U. Tumi, N. I. Shatskii, A. M. Cherepashchuk, S. A. Lamzin, and A. A. Belinskii, *Astrophys. Byull.* **72**, 382 (2017).
35. S. Potanin, A. Belinski, A. Dodin, et al., arXiv eprints, arXiv:2011.03061v1 (2020).
36. A. Preite-Martinez, A. Acker, J. Köppen, and B. Stenholm, *Astron. Astrophys. Suppl. Ser.* **88**, 121 (1991).
37. Ph. Prugniel, C. Soubiran, M. Koleva, and D. Le Borgne, arxiv: astro-ph/0703658 (2007).
38. C. Quireza, H. J. Rocha-Pinto, and W. J. Maciel, *Astron. Astrophys.* **475**, 217 (2007).
39. N. Sanduleak, private commun. (1984).
40. G. Schaller, D. Schaerer, G. Meynet, and A. Maeder, *Astron. Astrophys. Suppl. Ser.* **96**, 269 (1992).
41. B. J. Shappee, J. L. Prieto, D. Grupe, C. S. Kochanek, K. Z. Stanek, and G. de Rosa, *Astrophys. J.* **788**, 48 (2014).
42. P. J. Storey and D. G. Hummer, *Mon. Not. R. Astron. Soc.* **272**, 41 (1995).
43. V. L. Straizys, *Multicolor Stellar Photometry* (Mokslas, Vilnius, 1979; Pachart, Tucson, 1992).
44. V. L. Straizys, *Stars with Metal Deficite* (Mokslas, Vil'nyus, 1982) [in Russian].
45. F. Thévenin and G. Jasiewicz, *Astron. Astrophys.* **320**, 913 (1997).
46. R. Tylenda, A. Acker, B. Stenholm, and J. Köppen, *Astron. Astrophys. Suppl. Ser.* **95**, 337 (1992).
47. P. A. Whitelock, *Mon. Not. R. Astron. Soc.* **213**, 59 (1985).

Translated by V. Astakhov